Infrared cavity ringdown spectroscopy of methanol clusters: Single donor hydrogen bonding

R. A. Provencal, J. B. Paul,[a] K. Roth, C. Chapo, R. N. Casaes, and R. J. Saykally
Department of Chemistry, University of California, Berkeley, California 94720

G. S. Tschumper[b] and H. F. Schaefer III
Center for Computational Quantum Chemistry, University of Georgia, Athens, Georgia 30602-2525

(Received 22 September 1998; accepted 30 November 1998)

Infrared cavity ringdown laser absorption spectroscopy has been used to study the O–H stretching vibrations of jet-cooled methanol clusters in direct absorption. Rovibrational bands for $(CH_3OH)_2$, $(CH_3OH)_3$, and $(CH_3OH)_4$ have been measured. Both bonded and free O–H stretches were measured for the dimer, indicating that its structure is linear. Five bands were assigned to the methanol trimer, indicating the presence of a second cyclic isomer in the molecular beam. A detailed study of the free O–H stretching region shows that methanol clusters larger than dimer must exist in cyclic ring configurations. In order to facilitate spectral assignment, harmonic frequencies and infrared intensities were calculated for the methanol monomer, dimer, and trimer with second order Møller–Plesset perturbation theory. Using the theoretical infrared intensities and measured vibrational band absorptions, absolute cluster concentrations were calculated. Results agree with previous experimental and theoretical work. © *1999 American Institute of Physics.*
[S0021-9606(99)01809-7]

I. INTRODUCTION

Recent experimental and theoretical studies have provided much insight into the structures and hydrogen bond rearrangement dynamics of small water clusters.[1–6] Small water clusters have been shown to adopt quasiplanar homodromic ring structures and to undergo complex tunneling motions involving delocalization over numerous degenerate minima. Computer simulations have shown similar ring topologies to be important structural elements in the hydrogen bond network of liquid water. Clusters of methanol, the smallest organic compound which exhibits hydrogen bonding, provide the opportunity to study the changes in structure and hydrogen bonding effected by the replacement of a hydrogen with a methyl group, ostensibly forcing the system into exclusively single donor configurations.

Several groups have carried out *ab initio* calculations on methanol clusters. Recently, Buck *et al.* performed *ab initio* calculations on small methanol clusters using an intermolecular potential based essentially on SCF monomer wave functions.[7] Their results show that the lowest energy configuration of the methanol dimer is linear, while the most stable structures for clusters from the trimer to the decamer are monocyclic rings. In addition, Buck *et al.* calculated the frequency shift of the donor O–H stretch modes relative to those of the monomer for clusters up to decamer.[7] Vibrational spectra of the C═O and O–H stretch modes were calculated in the harmonic and anharmonic approximations using both second order perturbation theory as well as a variational approach. Their results reproduce experimental spectra for the dimer, but the trimer required a variational calculation explicitly including Darling–Dennison resonance terms to reproduce the observed spectrum. The potential energy surface of the methanol trimer has been investigated previously by Mó *et al.*[8] Using both SCF-CI and density functional methods, they also conclude that the trimer global minimum is a homodromic structure with two methyl groups on one side of the O–O–O plane and the third methyl on the other side. Their calculations also suggest that the bowl conformer, with all of the methyl groups on the same side of the O–O–O plane, is a minimum on the potential surface situated 0.8 kcal/mole above the global minimum. More recently, density functional calculations performed by Hagemeister *et al.* on methanol clusters up to the pentamer using the B3LYP functional similarly predict the lowest energy configurations to be linear for the dimer and cyclic for the trimer through pentamer.[9] Furthermore, Hagemeister *et al.* investigated chain and branched hydrogen bonded structures for these clusters. Their results showed that chain structures are destabilized due the combined effects of the loss of a hydrogen bond and the decrease in cooperative strength of the remaining hydrogen bonds. Branched structures result in a strengthening of the branch point methanol H-bond donation to its neighbor while simultaneously weakening its two acceptor H bonds.[9]

Experimentally, Huisken and co-workers[10] have studied the dissociation of methanol clusters with IR-molecular beam depletion spectroscopy. Upon excitation of the O–H stretch at 2.7 μm, they were able to measure dissociation spectra of the dimer and the trimer. The dimer spectrum consisted of absorption features at 3574 and 3684 cm^{-1}, assigned to the proton donor and acceptor O–H stretch bands, respectively. Buck and Ettischer have more recently mea-

[a]Present address: Harvard University, Department of Chemistry and Chemical Biology, Cambridge, MA 02138.
[b]Electronic mail: tschumpr@atossa.ccqc.uga.edu

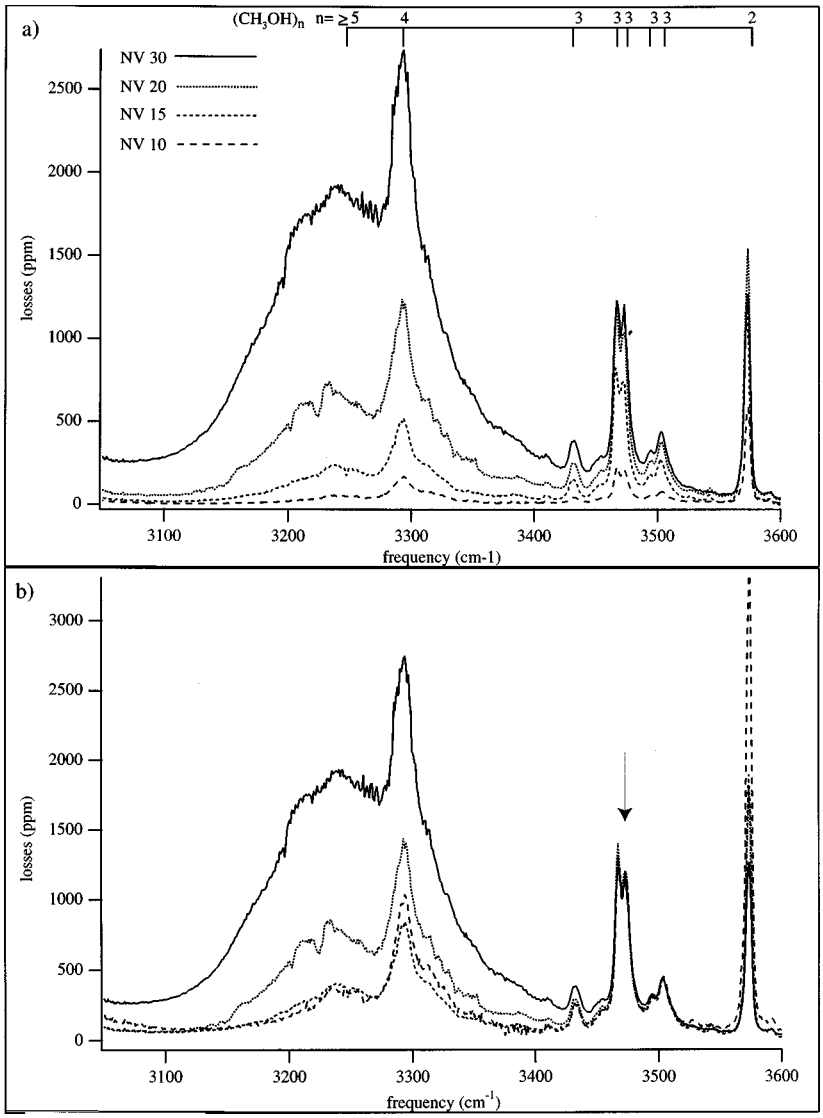

FIG. 1. Typical IR-CRLAS spectra of gas phase methanol clusters. (a) A series of scans taken at various methanol concentrations. Total source pressure is held constant for each scan, while the methanol concentration is controlled by use of a needle valve. Larger needle valve settings corresponds to higher methanol concentration. (b) Same spectra normalized to trimer feature at 3467 cm^{-1}. Bands not changing in intensity with respect to this feature can be assigned to the trimer, while bands that increase (decrease) in intensity with methanol concentration can be assigned to larger (smaller) clusters.

sured vibrational predissociation spectra in the O–H stretch region of $(CH_3OH)_n$ for n as large as nine.[11] Their measured spectra show redshifts as large as 500 cm^{-1}, but also exhibit an alteration between structured and unstructured spectra for odd and even clusters, respectively. Their calculations with a new potential model were able to reproduce the general features of the spectra but were unable to reproduce the observed red shifts. Lovas *et al.* have measured the microwave spectrum of the methanol dimer using a pulsed-beam Fabry–Perot Fourier transform microwave spectrometer.[12,13] Their recent results reveal that the $R(j)$ $K_a=0$ level is split into 15 states due to tunneling motions, while the $K_a=1$ level is split into 16 tunneling states. They also measured the barrier to internal rotation for the donor and acceptor methyl groups to be 180 and 120 cm^{-1}, respectively. The hydrogen bond distance was measured to be 1.96 (2) Å and the tilt of the acceptor methanol from the O–H–O axis was determined to be 77°.

Methanol clusters have also been studied extensively using matrix isolation infrared spectroscopy. For instance, Coussan *et al.* studied infrared laser induced isomerization of methanol polymers trapped in a nitrogen matrix.[14,15] By examining the effects of selective vibrational excitations of the O–H stretching modes on vibrational band intensities, they were able to deduce the sizes and structures of the carrier clusters. A detailed study of the 3370–3500 cm^{-1} region shows one broad transition due to a cyclic trimer species at 3450 cm^{-1}. Irradiation of this band leads to a ring opening and the appearance of several open chain trimer species. Annealing of the matrix reveals that a second cyclic trimer isomer also exists. From the differences in the C═O stretching spectrum of the two conformers, Coussan *et al.* deduce that these two isomer differ by position of the C═O bonds with respect to the plane defined by the three oxygen atoms.

Infrared cavity ringdown laser absorption spectroscopy (IR-CRLAS),[16] pioneered by Scherer *et al.*, has been shown to be a very useful technique for the study of structures and hydrogen bond rearrangement dynamics in hydrogen bonded systems.[17–20] Recently, Paul *et al.* used IR-CRLAS to study the O–D stretching region of gaseous D_2O clusters for the first time.[18] Using this technique, rovibrational bands for clusters as large as the D_2O hexamer have been measured, including rotationally resolved D_2O dimer spectra.[18,19] In this article, we report the results of an IR-CRLAS study of hy-

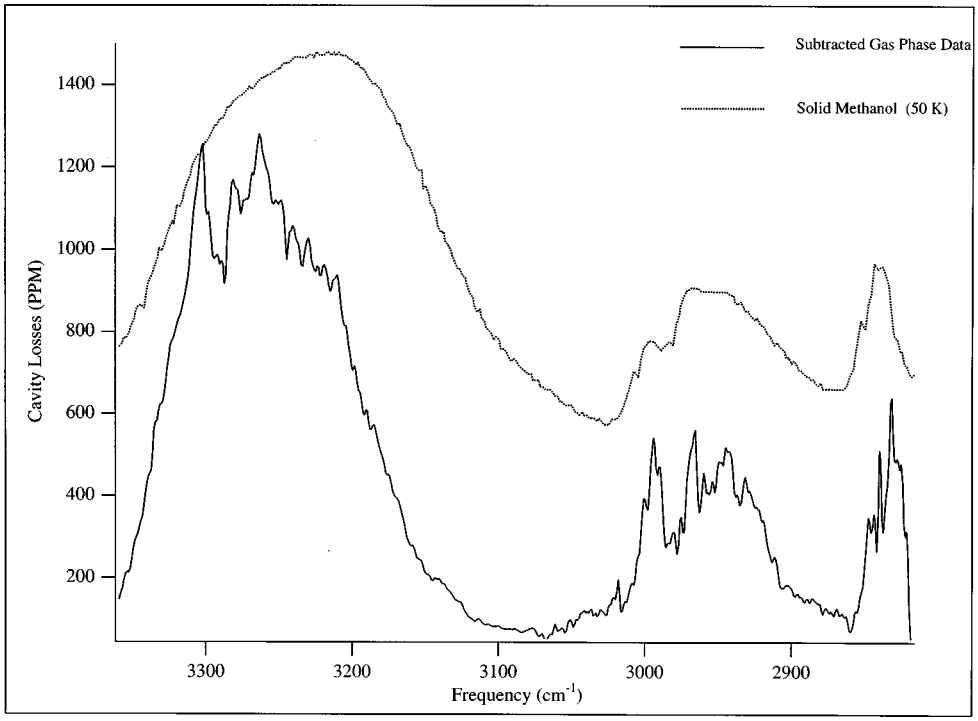

FIG. 2. Scans at high methanol concentrations reveal a broad feature due to large methanol clusters. The ringdown data shown here is the difference of the two highest concentration needle valve scans in Fig. 1 (NV20 and NV30). The dashed line is the spectrum of amorphous solid methanol at 50 K from Ref. 15. The general features of the solid methanol spectrum are very well reproduced. From this agreement, it is clear that our pulsed supersonic source produces clusters large enough to exhibit bulk like properties.

drogen bonded methanol complexes. Similar results for ethanol and butanol clusters will be the subject of future papers. Distinct rovibrational bands for methanol clusters as large as the tetramer have been measured, in addition to a broad methanol ''ice'' feature similar to that found in our water studies. Analysis of the data indicates that the dimer exists in a linear configuration, while all larger clusters must exist as monocyclic ring structures. Detailed study of the methanol trimer bands are in agreement with previous measurements of Huisken[10] and Buck,[11] but also suggest the possibility of more than one cyclic trimer isomer being present in the molecular beam. For comparison, we also report the results of theoretical calculations on small methanol clusters at the MP2 level of theory. The availability of the ab initio infrared intensities has also allowed us to deduce the absolute concentrations of methanol clusters present in the molecular beam.

II. EXPERIMENT

The Berkeley IR-CRLAS spectrometer used to obtain the present results has been described in recent publications.[18–20] Briefly, tunable infrared radiation was generated by Raman shifting a Nd:YAG (Continuum NY 82) pumped pulsed dye laser (Lambda Physik FL3002e). The Raman shifter consisted of a 3.5 m high-pressure multipass cell (Herriot configuration) containing 150 psi of H_2. After 17 passes, the 20–25 mJ/pulse of fundamental radiation (617–650 nm) generated 0.2–0.5 mJ/pulse of infrared (2.7–3.4 μm) in the third Stokes band. This tunable infrared radiation was then injected into the ringdown cavity, consisting of a pair of highly reflective dielectric mirrors ($R \sim 0.9999$). The light exiting the cavity through the second mirror was focused with a 10 cm lens onto a 0.5 mm diameter LN_2-cooled InSb detector. A 1 MHz bandwidth amplifier contained within the detector housing amplified the resulting signal. This signal was then digitized, averaged (20 shots/wavelength), and sent to a computer for least-squares fitting to a first-order exponential decay. The cavity optical transit time divided by the measured decay time yields the per-pass total cavity loss, which is recorded as a function of wavelength. The methanol clusters are produced by bubbling helium carrier gas through methanol and expanding the resultant mixture into a vacuum chamber through a 4 in. pulsed supersonic slit source, which generally produces clusters with rotational temperatures near 5 K. A background pressure of ~200 mTorr was maintained during the 40 Hz operation of the supersonic beam source by a 2500 cfm Roots pump. In order to obtain measurable ringdown times, we found it necessary to limit the number of large clusters formed in the expansion. This was done by seeding a higher pressure He/CH_3OH mixture into a lower pressure pure He flow through a needle valve, allowing precise control over the methanol concentration in the expansion, while maintaining a high overall source backing pressure of 35 psia. The data were wavelength calibrated from atmospheric water monomer transitions measured simultaneously with the methanol data, which provided an accuracy of 0.1 cm^{-1}.

III. THEORETICAL METHODS

Ab initio computations were carried out on the methanol monomer, dimer, and trimer. Equilibrium geometries, harmonic vibrational frequencies, and infrared (IR) intensities were determined for these three species using second order Møller–Plesset perturbation theory (MP2).[21] For all computations, the 1*s*-like orbitals on all C and O atoms were constrained to be doubly occupied. Similarly, the corresponding 1*s**-like virtual orbitals were deleted from the correlation procedure. As a measure of the validity of the frozen core

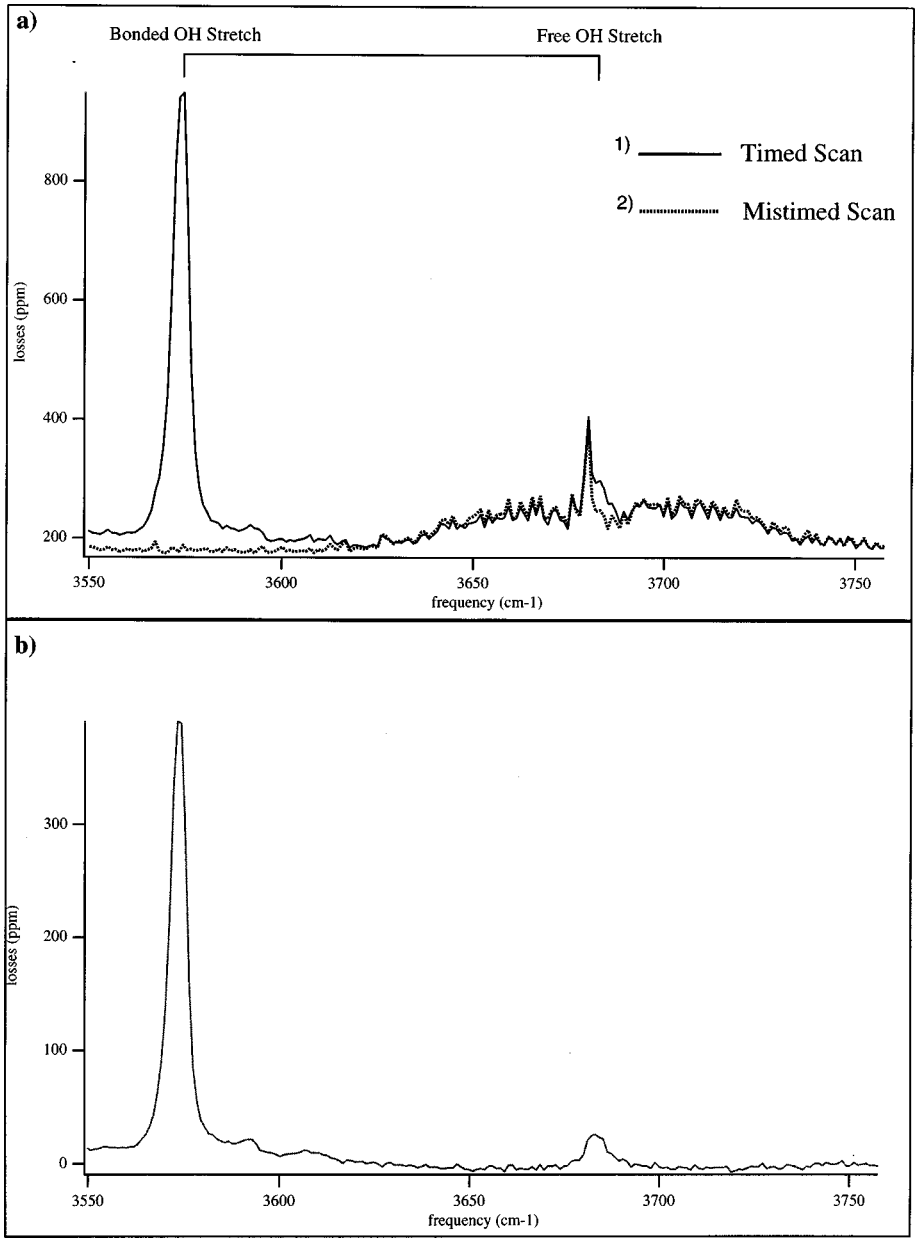

FIG. 3. IR-CRLAS spectra of the free O–H stretch region of methanol clusters. (a) Scan 1 is obtained with the molecular beam and ringdown pulse in phase with each other while scan 2 is obtained with the two out of phase. The in-phase scan probes both molecular beam and background chamber gas, while the out of phase scan probes only the background chamber gas (presumably monomer). (b) The difference between scan 1 and scan 2. This background subtraction method reveals a small absorption feature due to the free O–H stretch of the methanol dimer. Lack of free O–H bands due to larger clusters implies that all clusters larger than the dime must exist in cyclic configurations.

approximation, computations in which all electrons and virtual orbitals were included were carried out on the trimer with the smaller of the two basis sets employed. The properties of interest were quite insensitive to such changes in the correlation procedure. All *ab initio* computations were carried out using the GAUSSIAN 94[22] system of programs. Elements of the density matrices were converged to six decimal places while the root mean square of these elements was converged to eight decimal places. This resulted in total energies that were converged to at least 1×10^{-7} hartree.

Two double-ζ basis sets with polarization functions, denoted DZP and DZP++, were employed—the latter being augmented with diffuse functions. The DZP basis was constructed from the Huzinaga–Dunning[23,24] set of contracted double-ζ Gaussian functions with the addition of one set of *p*-type polarization functions for each H atom with orbital exponent $\alpha_p(\mathrm{H})=0.75$ and one set of five *d*-type polarization functions for each C and O atom with orbital exponents $\alpha_d(\mathrm{C})=0.75$ and $\alpha_d(\mathrm{O})=0.85$. To form the DZP++ basis, one even tempered *s*-type diffuse function was added to each H atom $\alpha_s(\mathrm{H})=0.04415$, and a set of even tempered *s*- and *p*-type diffuse functions were added to each C and O atom, $\alpha_s(\mathrm{C})=0.04302$, $\alpha_p(\mathrm{C})=0.03629$, $\alpha_s(\mathrm{O})=0.08227$, and $\alpha_p(\mathrm{O})=0.06508$.[25] The designation for the DZP++ basis set is thus C,O $(10s6p1d/5s3p1d)$, H$(5s1p/3s1p)$.

For each basis set, equilibrium geometries, harmonic vibrational frequencies, and infrared (IR) intensities were determined using the available analytic MP2 gradients and second derivatives in the GAUSSIAN 94[22] program package. The monomer was optimized in the C_s symmetry while no symmetry constraints were placed upon the dimer and trimer. Although several optimized geometrical parameters of the dimer and trimer appear identical to the precision reported, they were not constrained to be so. Residual Cartesian forces of the reported equilibrium structures were less than 1.0

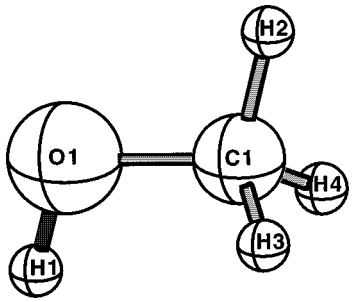

FIG. 4. C_s equilibrium structure of CH_3OH. O_1, C_1, H_1, and H_2 lie in the plane of symmetry. H_4 can be generated from H_3 by reflection through the plane of symmetry.

$\times 10^{-6}$ hartree/Bohr. It is important to reiterate that the computed vibrational frequencies are harmonic in nature and the corresponding IR intensities were determined within the double harmonic approximation. Due to the floppy nature of the $(CH_3OH)_2$ and $(CH_3OH)_3$, care must be exercised when comparisons are made between these theoretical values and those obtained from experiment.

IV. RESULTS

A. Experiment

Typical IR-CRLAS spectra of jet cooled methanol are shown in Fig. 1(a). The spectra were obtained using a constant source backing pressure and thus nearly constant beam expansion temperature, while the methanol concentration was varied with a needle valve. Several distinct cluster bands can be seen as well as an underlying broad absorption feature which appears at larger methanol concentrations. The carriers of these bands can be identified by measuring the relative change of band absorption as a function of increasing methanol concentration, assuming the temperature of the molecular beam to be constant. Figure 1(b) shows the same spectra in Fig. 1(a) normalized to the methanol trimer bands, wherein the strong peak at 3574.4 cm^{-1} decreases in intensity with increasing methanol concentration, while the bands to the red increase with increasing methanol concentration. This implies that the 3574.4 cm^{-1} band is due to a smaller cluster (i.e., the dimer), while the bands shifted to the red are from larger clusters (i.e., tetramer and larger). Following this procedure, we can assign the 3574.4 band to the methanol dimer. Five bands can be assigned to the trimer, including two stronger bands of nearly equal intensity at 3473.2, 3467.1, and three weaker bands at 3503.7, 3494.6, and 3432.1. The 3278.5 band can be assigned to the tetramer, while the broad feature that appears at highest methanol concentrations is due to larger clusters. This feature is very similar to those found in our previous studies on water clusters, which shows a large absorption feature due to amorphous ice.[20] Figure 2 shows the comparison of our methanol data with the spectrum of amorphous solid methanol at 50 K.[26] The methanol data shown in Fig. 2 represent the difference between the two scans with the highest methanol concentrations. The general features of the spectrum of solid methanol are well reproduced. This implies that at higher methanol concentrations, large clusters are produced which exhibit the properties of disordered solid methanol.

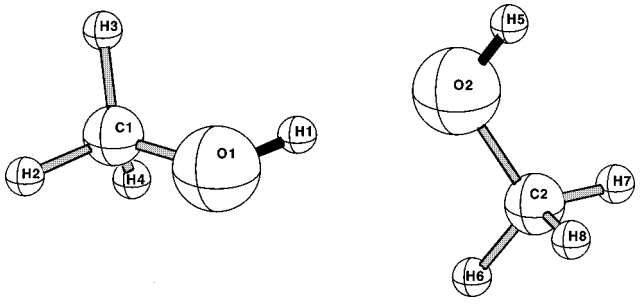

FIG. 5. Equilibrium structure of $(CH_3OH)_2$.

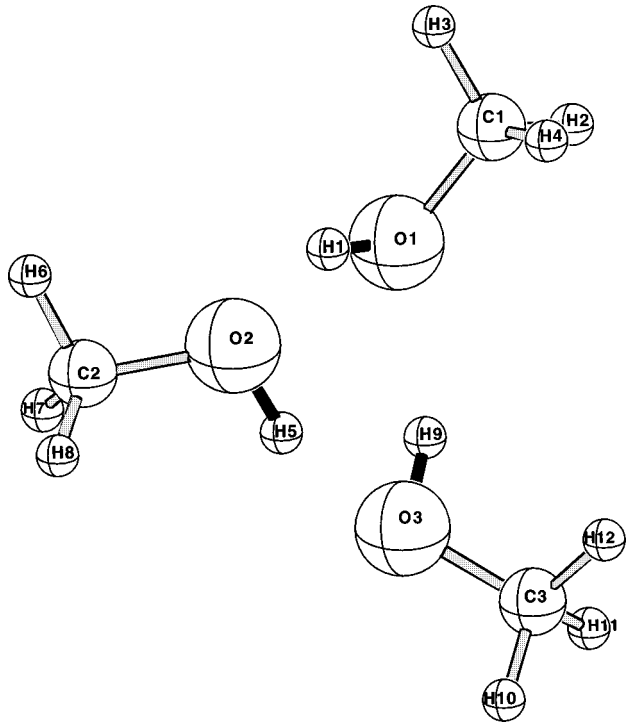

FIG. 6. Equilibrium structure of $(CH_3OH)_3$.

Additional structural information can also be extracted from our data by closely examining the free O–H stretching region at 3681 cm^{-1}. In addition to the free O–H stretch of the methanol monomer, we would also expect to see the free O–H stretches of any cluster molecules having a free O–H. To determine if such features are present, it is necessary to differentiate cluster peaks from monomer transitions measured both in the molecular beam and also those absorbing in the chamber background gas. This is accomplished by performing a series of scans at various methanol concentrations. For a given methanol concentration, two scans are obtained. In the first scan, the molecular beam and the ringdown pulse are timed to be in phase with each other, thus probing both the molecular beam and background gas. In the second, the two are timed out of phase with respect to each other, thus probing only the background gas. Subtraction of these two scans removes background gas absorptions, leaving only transitions measured in the molecular beam. Figure 3 illustrates an example of this background subtraction technique.

TABLE I. Equilibrium properties of the CH_3OH monomer, dimer, and trimer at the MP2 level of theory with the DZP++ basis set. The energies (E_{SCF} and E_{MP2}) are given in hartrees, bond lengths (r_{XY}) in Å, bond angles (θ_{XYZ}), in degrees, and torsional angles (τ_{WXYZ}) in degrees. The atom numbers correspond to those found in Figs. 4, 5, and 6.

Parameter	Monomer	Dimer	Trimer
E_{SCF}	−115.07435	−230.15525	−345.24091
E_{MP2}	−115.41057	−230.83247	−346.26400
	Intramolecular Parameters		
$r_{O_1H_1}$	0.969	0.976	0.984
$r_{C_1O_1}$	1.429	1.423	1.429
$r_{C_1H_2}$	1.092	1.094	1.093
$r_{C_1H_3}$	1.099	1.100	1.098
$r_{C_1H_4}$	1.099	1.100	1.099
$\theta_{C_1O_1H_1}$	107.7	107.2	108.4
$\theta_{C_1O_1H_2}$	106.4	107.2	107.2
$\theta_{C_1O_1H_3}$	111.9	112.0	111.2
$\theta_{C_1O_1H_4}$	180.0	112.1	111.7
$\tau_{H_1O_1C_1H_2}$	−61.4	178.5	177.8
$\tau_{H_1O_1C_1H_3}$	61.4	−62.6	−63.5
$\tau_{H_1O_1C_1H_4}$		59.7	58.5
$r_{O_2H_5}$		0.970	0.983
$r_{C_2O_5}$		1.437	1.430
$r_{C_2H_6}$		1.092	1.093
$r_{C_2H_7}$		1.097	1.098
$r_{C_2H_8}$		1.097	1.098
$\theta_{C_2O_2H_5}$		108.2	108.4
$\theta_{O_2C_2H_6}$		106.2	107.2
$\theta_{O_2C_2H_7}$		111.2	111.5
$\theta_{O_2C_2H_8}$		111.5	111.1
$\tau_{H_5O_2C_2H_6}$		178.4	−177.4
$\tau_{H_5O_2C_2H_7}$		−62.9	−58.1
$\tau_{H_5O_2C_2H_8}$		59.9	63.9
$r_{O_3H_9}$			0.983
$r_{C_3O_3}$			1.429
$r_{C_3H_{10}}$			1.093
$r_{C_3H_{11}}$			1.098
$r_{C_3H_{12}}$			1.099
$\theta_{C_3O_3H_9}$			108.6
$\theta_{C_3O_3H_{10}}$			107.2
$\theta_{C_3O_3H_{11}}$			111.2
$\theta_{C_3O_3H_{12}}$			111.7
$\tau_{H_6O_3C_3H_{10}}$			177.6
$\tau_{H_6O_3C_3H_{11}}$			−63.6
$\tau_{H_6O_3C_3H_{12}}$			58.5
	Intermolecular Parameters		
$r_{H_1O_2}$		1.872	1.839
$r_{H_5O_3}$			1.845
$r_{H_9O_1}$			1.868
$r_{O_1O_2}$		2.842	2.750
$r_{O_1O_3}$			2.764
$r_{O_2O_3}$			2.748
$\theta_{O_1H_1O_2}$		172.1	152.4
$\theta_{O_2H_5O_3}$			151.2
$\theta_{O_3H_9O_1}$			150.0
$\theta_{O_1O_2O_3}$			60.4
$\theta_{O_2O_3O_1}$			59.9
$\theta_{C_2O_2H_1}$		110.3	
$\tau_{O_2H_1O_1C_1}$		−97.4	
$\tau_{O_1H_1O_2C_2}$		−23.4	
$\tau_{O_1H_1O_2H_5}$		−149.3	
$\tau_{H_1O_1O_2O_3}$			174.9
$\tau_{H_5O_2O_3O_1}$			−175.2
$\tau_{H_9O_3O_1O_2}$			−179.8
$\tau_{C_1O_1O_2O_3}$			−121.5
$\tau_{C_2O_2O_3O_1}$			117.1
$\tau_{C_3O_3O_1O_2}$			−118.4

TABLE II. Harmonic vibrational frequencies and infrared (IR) intensities of CH_3OH monomer, dimer, and trimer at the MP2 level of theory with the DZP++ basis set. Frequencies (in cm^{-1}) are ordered in decreasing frequency. Infrared intensities (in km/mol) are listed in parentheses.

Mode	Monomer		Dimer		Trimer	
ω_1	3889	(32)	3879	(44)	3645	(796)
ω_2	3227	(30)	3735	(494)	3633	(848)
ω_3	3160	(62)	3240	(20)	3564	(27)
ω_4	3076	(69)	3206	(47)	3218	(52)
ω_5	1530	(4)	3188	(41)	3218	(22)
ω_6	1515	(2)	3138	(72)	3215	(33)
ω_7	1500	(9)	3094	(57)	3169	(51)
ω_8	1370	(19)	3060	(86)	3165	(54)
ω_9	1181	(0)	1530	(5)	3163	(50)
ω_{10}	1090	(11)	1529	(2)	3080	(30)
ω_{11}	1064	(116)	1519	(3)	3077	(147)
ω_{12}	306	(131)	1513	(1)	3075	(702)
ω_{13}			1501	(4)	1535	(1)
ω_{14}			1498	(15)	1533	(3)
ω_{15}			1444	(26)	1532	(4)
ω_{16}			1372	(24)	1520	(0)
ω_{17}			1186	(1)	1520	(3)
ω_{18}			1181	(1)	1519	(4)
ω_{19}			1126	(9)	1506	(7)
ω_{20}			1093	(95)	1497	(13)
ω_{21}			1085	(8)	1496	(4)
ω_{22}			1064	(148)	1482	(12)
ω_{23}			729	(108)	1444	(97)
ω_{24}			362	(113)	1432	(77)
ω_{25}			200	(1)	1188	(2)
ω_{26}			116	(1)	1188	(1)
ω_{27}			106	(3)	1187	(1)
ω_{28}			54	(13)	1169	(1)
ω_{29}			47	(5)	1140	(35)
ω_{30}			29	(9)	1128	(23)
ω_{31}					1096	(16)
ω_{32}					1083	(208)
ω_{33}					1081	(147)
ω_{34}					872	(30)
ω_{35}					742	(256)
ω_{36}					662	(189)
ω_{37}					220	(4)
ω_{38}					216	(3)
ω_{39}					197	(7)
ω_{40}					170	(3)
ω_{41}					115	(1)
ω_{42}					111	(1)
ω_{43}					109	(0)
ω_{44}					93	(13)
ω_{45}					83	(12)
ω_{46}					54	(5)
ω_{47}					38	(3)
ω_{48}					30	(6)

Scan 1 in Fig. 3(a) was obtained with the valve and CRLAS probe operating in phase, while Scan 2 was obtained with the two out of phase. The difference between these two scans, shown in Fig. 3(b), reveals a small absorption feature blue shifted from the monomer transition by 2.3 cm^{-1}. Repetition of this procedure at several methanol concentrations shows that this weak feature normalizes to the dimer, in agreement with theoretical calculations.[9] No evidence for the free O–H groups of any larger clusters was apparent.

TABLE III. Comparison of this work with previous experimental and theoretical results. Frequencies are given in wavenumbers and intensities in (km/mol).

	Experimental		Theoretical				
	This work	Huisken[a]	This work		Buck *et al.*[b]	Mó *et al.*[c]	Hagemiester *et al.*[d]
			DZP++		[e]	[f] [g]	
$(CH_3OH)_2$	3683.8	3684.1	3879	(44)	3641	3843	3759
	3574.4	3574.4	3735	(494)	3519	3091	3613
$(CH_3OH)_3$	3503.7	3503.4				3625	
	3494.6					3623	
	3473.2	3471.8	3645	(796)	3494	3612	3535
	3467.1		3633	(848)	3487	3600	3521
	3432.1	3433.6	3565	(26)	3456	3546	3465
$(CH_3OH)_4$	3278.5				3378		3392

[a]Reference 10.
[b]Reference 7.
[c]Reference 8.
[d]Reference 9.
[e]Harmonic approximation.
[f]Asymmetric isomer.
[g]Bowl isomer, assignment tentative.

B. Theory

For brevity, only the results obtained with the largest basis set (DZP++) are reported. Data from the smaller DZP basis are available upon request. The equilibrium structures of the methanol monomer, dimer, and trimer obtained with the DZP++ basis set are shown in Figs. 4, 5, and 6 respectively. Note the numbering of the H atoms in each methanol moiety. For each monomeric subunit, if H_n is bonded to O, then H_{n+1} is bonded to C and makes a torsional angle with H_n about the O–C bond ($\tau_{H_nOCH_{n+1}}$) of approximately 180°. H_{n+2} and H_{n+3} are also bonded to C. The analogous torsional angles are near ±60°. The torsion about the C–O bond is always counterclockwise for $\tau_{H_nOCH_{n+2}}$ (−60°) and clockwise for $\tau_{H_nOCH_{n+3}}$ (60°). Table I contains the optimized geometrical parameters for the monomer, dimer, and trimer. Since these results provide an excellent starting point for higher level theoretical investigations of $(CH_3OH)_2$ and $(CH_3OH)_3$, some redundancies are included in the reported geometrical parameters in order to facilitate reproduction of a Cartesian or *Z*-matrix, something that has been lacking in the literature until now.

In the minimum energy dimer structure (see Fig. 5) the three atoms forming the hydrogen bond angle (O_1, H_1, and O_2) will be used to define an arbitrary plane for reference (approximately the plane of the paper) and H_5 are all quasiplanar. The atom C_2, lies very nearly in this $O_1\cdots H_1\cdots O_2$ plane. On the other hand, H_5 resides ''above'' this plane while C_1 lies significantly ''below'' it.

The three O atoms of the methanol trimer (see Fig. 6) form a convenient plane of reference, approximately the plane of the paper. While the hydroxyl H atoms are nearly in the plane of the O atoms, the methyl carbons are bent significantly out of the plane. The DZP++ (DZP) equilibrium structure places the two of the carbon atoms ''below'' (C_1 and C_3) and one ''above'' (C_2) the $O_1\cdots O_2\cdots O_3$ plane. All three hydroxyl H atoms, on the other hand, lie essentially in this plane.

The harmonic vibrational frequencies and IR intensities are reported in Table II for the monomer, dimer, and trimer. The frequencies are listed in order of decreasing magnitude.

V. DISCUSSION

Table III summarizes the present results and compares them with previous experiments and theoretical predictions. Overall, our work agrees well with both. For the methanol dimer, the molecular beam depletion experiments of Huisken and Stemmler[27] revealed two bands, corresponding to completely local modes of methanol acceptor free O–H stretch and a donor bonded O–H stretch. Our experimental results also reveal two similar features assignable to the methanol dimer, in agreement with Huisken. Our calculations on the methanol dimer (see Table II) at the MP2 level of theory predict two bands in the O–H stretch region, at 3887 and 3746 cm^{-1}, with an approximate bonded:free intensity ratio of 1:10. Scaling these harmonic values by the usual 0.95, gives frequencies of 3692 and 3559 cm^{-1}. This good agreement indicates that the methanol dimer is present in a linear hydrogen-bonded configuration. It is interesting to note that the free O–H stretch of the dimer is actually blue shifted relative to the monomer. This is undoubtedly due to the decrease in O–H bond length that occurs upon electron donation to the hydrogen bond. It is also noteworthy that the only cluster band measured in the free O–H stretch region was that of the dimer. The lack of free O–H bands of larger clusters establishes that all clusters larger than the dimer must exist as cyclic ring structures, with all O–H's explicitly involved in hydrogen bonding.

Huisken *et al.* also performed an experimental investigation of the O–H stretching region of the methanol trimer.[10] Figure 7 compares the results of Huisken *et al.* with those presented here. He found three trimer O–H stretch bands, a strong peak at 3471.8 and two weaker features at 3503.4 and 3433.6 cm^{-1}. The higher resolution of our experiment (~.2 cm^{-1} vs 2 cm^{-1}) allows us to determine that the strong feature at 3471.8 is actually consists of two peaks of almost equal intensity, separated by 6.1 cm^{-1}. Our calculations at

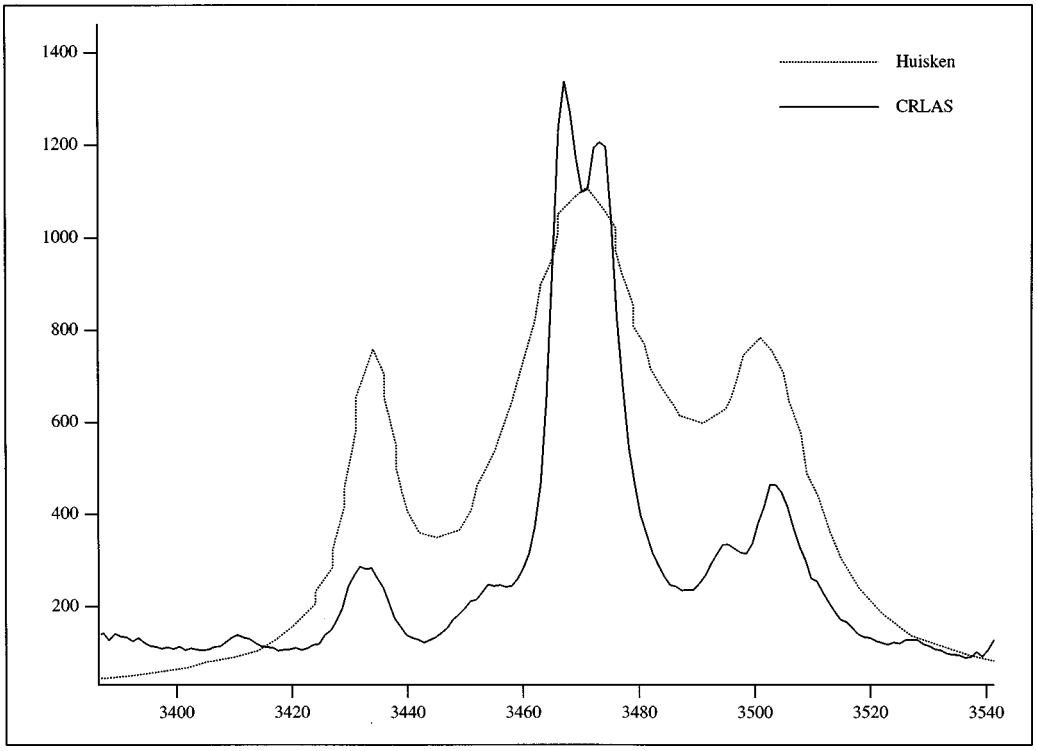

FIG. 7. Comparison of CRLAS scans in the bonded O–H stretch region of the methanol trimer with the results of Huisken *et al.* (Ref. 10). It is clearly seen that the peak measured by Huisken *et al.* at 3470 cm^{-1} is split into to peaks of nearly equal intensity. The peak at 3503 cm^{-1} is also split into two peaks, a stronger peak at 3503.7 and a weaker feature at 3494.6 cm^{-1}. The presence of more than three peaks assignable to the trimer implies that two methanol trimer conformers coexist in the molecular beam. The peaks at 3473.2, 3467.1, and 3232.1 cm^{-1} can be assigned to the asymmetric cyclic trimer, while the peaks at 3503.7 and 3494.6 cm^{-1} are tentatively assigned to the bowl conformer, calculated to lie 0.8 kcal/mol above the asymmetric form.

the MP2 level of theory (see Table II) with a DZP++ basis set predict three bands in the O–H stretch region for the lowest energy structure of the methanol trimer at 3645, 3633, and 3565 cm^{-1} with relative intensity ratios of .94:1.0:.03, respectively. Scaled frequencies of 3462, 3451, and 3386 cm^{-1} match reasonably well with the experimental results. Because of the overlap of the two strongest peaks at 3473 and 3467, it is difficult to obtain an accurate relative intensity of these three peaks, although clearly the band at 3432 is more intense than predicted. Calculations at various other levels of theory[7–9] also predict that the cyclic methanol trimer spectrum should consist of three peaks, two of equal intensity separated by approximately 5–10 cm^{-1}, and another weaker band shifted to the red by 25–50 cm^{-1}. As a result of this agreement between our work and theoretical predictions, we assign the bands measured at 3473.2, 3467.1, and 3432.1 to the cyclic methanol trimer. These vibrational modes correspond to linear combinations of the three O–H stretches of the methanol monomers. The two bands of nearly equal intensity can be thought of as antisymmetric combinations, while the weaker mode can be considered an almost totally symmtric combination. Assignment of the 3503 and the 3496 cm^{-1} bands, which also normalize to a trimer structure, is more speculative. The presence of more than three peaks assignable to the trimer implies that more than one conformer could be present in the molecular beam. The lack of any free O–H stretching modes assignable to the trimer implies that, if these peaks are due to another trimer conformer, then it also must be a cyclic ring structure. The matrix work of Coussan[14] also shows the presence of two cyclic trimer isomers. While the O–H stretches of these two structures are comparable, the C═O frequencies of the two isomers show a much larger splitting for the most stable structure. This suggests that the conformers differ in the positions of the C═O bonds relative to the O–O–O plane. A recent study by Mó *et al.* shows that the bowl conformer of the methanol trimer with all methyl groups on the same side of the O–O–O plane is 0.8 kcal/mol above the global minimum. They also predict that the spectrum of the bowl conformer in the O–H stretching region should consist of three peaks at 3625, 3623, and 3574 cm^{-1}.[8] These peaks are shifted slightly to the blue relative to the cyclic structure. It is likely that the two peaks measured at 3503.7, and 3494.6 are due to bowl conformer. There is also a very weak feature at 3454.5 cm^{-1} which cannot be conclusively assigned as a trimer peak, but could certainly correspond to the third trimer bowl peak. Clearly, a detailed IR-CRLAS study of the C═O stretching region of methanol clusters is necessary once extension into this region of the spectrum is accomplished. It is also a possibility that the carrier of these transitions is not actually the trimer, but some other cluster. This seems unlikely due the agreement of our data with the work of Huisken *et al.*, who employs kinematic size selection in his technique. Huisken also measures a trimer feature at 3503 cm^{-1}, in agreement with our data. Due to the lower resolution of their experiment, they probably could not detect the weak feature at 3494 cm^{-1}. While the difference in energy between the two conformers is rather large when considering

the temperature of our molecular beam, it is possible the energy difference between these two conformers is much less than predicted by the DFT calculations of Mó. In any case, it is clear that the energetics of methanol trimer conformers needs further theoretical and experimental investigation.

It is also clear from this work that at high methanol concentrations, clusters larger than the trimer dominate the molecular beam. The strongest feature in the spectrum at high concentrations (see Fig. 1) can be assigned to a bonded O–H stretching vibration of the methanol tetramer. Remarkably, Weltner and Pitzer first speculated that the methanol tetramer may be stable in the gas phase based on their heat capacity measurements of gaseous methanol.[28] They interpreted a large nonlinear trend in the heat capacity as a function of pressure to indicated the presence of methanol tetramers in the gas. It is interesting to note that there is no methanol pentamer feature analogous to the water pentamer. This could imply that the methanol tetramer is most important structural element in bulk methanol. The tetramer is most likely favored over the pentamer due to the steric repulsion effected by having two methyl groups on the same side of the ring. Also appearing at high methanol concentrations is a broad O–H stretching feature which is due to clusters larger than the tetramer. This feature reproduces the spectrum of solid amorphous methanol,[26] as shown in Fig. 2. Luck *et al.* measured the spectrum of solid methanol at a variety of temperatures. As the solid is heated, the broad O–H stretching band of solid methanol shifts to the red. From a simple extrapolation, we can estimate the temperature of the ''solid-like'' clusters in our beam to be approximately 10 K. The structure of crystalline solid methanol has also been investigated by Tauer and Lipscomb.[29] From their x-ray studies, they show that the structure of crystalline methanol consists of a unit cell of four methanol molecules with an infinite chain of zigzag hydrogen bonds. Luck *et al.* also studied the spectrum of liquid methanol at a variety of temperatures. The liquid spectra consists of a broad featureless O–H stretching band centered near 3350 cm^{-1}. Clearly, liquid methanol displays the characteristics of a large cooperative hydrogen-bond network.

Previous work has shown that it is possible to extract absolute cluster concentrations from CRLAS data.[17] From the calculated theoretical intensities and measured integrated vibrational band absorptions, we are able to calculate the absolute concentrations of dimers and trimers in the molecular beam. The lack of accurate theoretical intensities for the tetramer obviate calculation of its concentration. Assuming that Beer's law applies, we calculate the concentration of dimers and trimers to be 1.3×10^{13} and 5.5×10^{12} mole/cm^3, respectively, with modest total methanol concentration. The total band intensities were calculated by fitting each rovibrational band to a Lorentzian lineshape. From the area of this peak, total integrated band absorptions were calculated. The calculated trimer concentration represents and average of the concentrations calculated from the two most intense trimer bands. While the uncertainties in these concentrations depend on the uncertainty in the vibrational band intensities, these results can best be viewed as a lower bound of the actual concentrations.

We can see from our studies of the free O–H stretch region (see Fig. 2) that methanol does not exist in its monomeric form in the molecular beam. The only monomer transitions measured were due to methanol in the background gas. While direct comparison with previous measurement on water clusters[17] is not possible due to differences in source conditions, one feature appears to be prominent. The concentration of the methanol dimer is approximately twice that of the trimer, whereas the trend for water clusters shows the trimer to be the dominant species. This most likely is due to differences in the kinetics of formation of methanol clusters. Unfortunately, the exact conditions used to acquire the water data could not be duplicated. The low vapor pressure of methanol made it necessary to control its concentration with a needle valve. Thus, the methanol data were obtained at constant backing pressure with various concentrations, while the water data was obtained as a function of increasing backing pressure without the use of a needle valve. Large absorptions ($>$3000 ppm) seen without the needle valve made obtaining methanol spectra as a function of source backing pressure unfeasible.

VI. SUMMARY

In this article, the results of our IR-CRLAS study of gas-phase methanol clusters have been presented. Vibrational bands for clusters as large as the methanol tetramer have been assigned. Vibrational bands at 3574.4 and 3683.8 cm^{-1} have been assigned to the bound and free O–H stretch vibrations of the linear methanol dimer, in agreement with theoretical calculations reported herein at the MP2 level of theory. Vibrational bands at 3473.2, 3467.1, and 3432.1 cm^{-1} can be assigned to the bound O–H stretches of the asymmetric cyclic methanol trimer. Two additional bands at 3503.7 and 3494.6 cm^{-1} can be also due to a cyclic trimer conformer, although it is not yet possible to determine the structure of carrier of these bands. The absence of a free O–H stretch assignable to the trimer indicates that this conformer must be cyclic, however. Theoretical predictions suggest that this could be the bowl conformer, but more theoretical and experimental work is necessary to confirm this assignment. At high concentrations of methanol, large clusters exhibiting bulk-like properties are seen. Our results also show that all clusters larger than the dimer must exist in cyclic configurations, with all O–H groups involved in the hydrogen bond network.

ACKNOWLEDGMENTS

The authors thank Dr. Arthur Suits for loaning the Raman shifter used in this work. This work is supported by the Air Force, Office of Sponsored Research (Grant No. F49620-96-1-0411) and the National Science Foundation (Grant Nos. CHE-952728 and CHE-9727302). R.A.P. is a NASA Graduate Student Researchers Program Fellow. C.C. is a National Science Foundation Fellow. R.J.S. is a UC-Berkeley Miller Research Professor 1997–1998.

[1] J. D. Cruzan, M. G. Brown, K. Liu, L. B. Braly, and R. J. Saykally, J. Chem. Phys. **105**, 6634 (1996).
[2] J. D. Cruzan, M. R. Viant, M. G. Brown, and R. J. Saykally, J. Phys. Chem. A **101**, 9022 (1997).
[3] K. Liu, J. D. Cruzan, and R. J. Saykally, Science **271**, 929 (1996).
[4] E. H. T. Olthof, A. Van der Avoird, P. E. S. Wormer, K. Liu, and R. J. Saykally, J. Chem. Phys. **105**, 8051 (1996).
[5] C. Leforestier, L. B. Braly, K. Liu, M. J. Elrod, and R. J. Saykally, J. Chem. Phys. **106**, 8527 (1997).
[6] J. K. Gregory and D. C. Clary, J. Phys. Chem. **100**, 18014 (1996).
[7] U. Buck, J. G. Siebers, and R. J. Wheatley, J. Chem. Phys. **108**, 20 (1998).
[8] O. Mó, M. Yanez, and J. Elguero, J. Chem. Phys. **107**, 3592 (1997).
[9] F. C. Hagemeister, C. J. Gruenloh, and T. S. Zwier, J. Phys. Chem. A **102**, 82 (1998).
[10] F. Huisken, M. Kaloudis, M. Koch, and O. Werhahn, J. Chem. Phys. **105**, 8965 (1996).
[11] U. Buck and I. Ettischer, J. Chem. Phys. **108**, 33 (1998).
[12] F. J. Lovas, S. P. Belov, M. Y. Tretyakov, W. Stahl, and R. D. Suenram, J. Mol. Spectrosc. **170**, 478 (1995).
[13] F. J. Lovas and H. Hartwig, J. Mol. Spectrosc. **185**, 98 (1997).
[14] S. Coussan, A. Loutellier, J. P. Perchard, S. Racine, A. Peremans, A. Tadjeddine, and W. Q. Zheng, J. Chem. Phys. **107**, 6526 (1997).
[15] S. Coussan, Y. Bouteiller, A. Loutellier, J. P. Perchard, S. Racine, A. Peremans, W. Q. Zheng, and A. Tadjeddine, Chem. Phys. **219**, 221 (1997).
[16] J. J. Scherer, D. Voelkel, D. J. Rakestraw, J. B. Paul, C. P. Collier, R. J. Saykally, and A. O'Keefe, Chem. Phys. Lett. **245**, 273 (1995).
[17] J. B. Paul, C. P. Collier, R. J. Saykally, J. J. Scherer, and A. Okeefe, J. Phys. Chem. A **101**, 5211 (1997).
[18] J. B. Paul, R. A. Provencal, and R. J. Saykally, J. Phys. Chem. A **102**, 3279 (1998).
[19] J. B. Paul, R. A. Provencal, C. Chapo, A. Pettersson, and R. J. Saykally, J. Chem. Phys. **109**, 10201 (1998).
[20] J. B. Paul, R. A. Provencal, C. Chapo, K. Roth, R. N. Casaes, and R. J. Saykally, J. Phys. Chem. A (submitted).
[21] C. Møller and M. S. Plesset, Phys. Rev. **46**, 618 (1934).
[22] M. J. Frisch *et al.*, GAUSSIAN 94, *Revision C*, 3rd ed. (Gaussian, Inc., Pittsburgh, PA, 1995).
[23] S. Huzinaga, J. Chem. Phys. **42**, 1293 (1965).
[24] T. H. Dunning, J. Chem. Phys. **53**, 1784 (1970).
[25] T. J. Lee and H. F. Schaefer, J. Chem. Phys. **83**, 1784 (1985).
[26] W. A. P. Luck and M. Fritzsche, Z. Phys. Chem. (Munich) **191**, 71 (1995).
[27] F. Huisken and M. Stemmler, J. Chem. Phys. **98**, 7680 (1993).
[28] W. Weltner and K. S. Pitzer, J. Am. Chem. Soc. **73**, 2606 (1951).
[29] K. J. Tauer and W. N. Lipscomb, Acta Crystallogr. **5**, 606 (1952).